

International Journal of Innovative Research in Science, Engineering and Technology

(A High Impact Factor, Monthly, Peer Reviewed Journal)

Visit: www.ijirset.com

Vol. 7, Issue 4, April 2018

Online Uninterruptible Power Supply with Transformerless Topology for Low Power Applications

Amit Kurmoli¹, Dr. S Sumathi²

M.Tech Student, Dept. of E&E, RNSIT, Bengaluru, India¹

HOD & Associate Professor, Dept. of E&E, RNSIT, Bengaluru, India²

ABSTRACT: An Uninterruptible Power Supply (UPS) provides nearly instantaneous power when the main utility power source fails, these are widely used to provide reliable and high quality power to critical loads in all grid conditions. This paper proposes a non-isolated online uninterruptible power supply (UPS) system. The proposed system consists of bridgeless PFC boost rectifier, battery charger/discharger, and an inverter. A new battery charger/discharger has been proposed which ensures the bidirectional power flow between dc-link and battery bank, reducing the battery bank voltage to only 24V, and regulates the dc-link voltage during power failure from the grid. A new control method, proportional-resonant control and integrating slide mode control, for inverter has been proposed which regulates the output voltage for both non-linear and linear loads. The controller exhibits excellent performance during step changes and transients in load.

KEYWORDS: Uninterruptible power supply, Battery charger/discharger, Power factor correction, Transformerless UPS

I. INTRODUCTION

Uninterruptible power supplies (UPS) provide clean, conditioned, and reliable power to critical loads such as communication systems, network servers, medical equipment's etc. in all grid conditions [1, 2]. Typically the UPS provides high efficiency, unity power factor, low cost, high reliability and low transients response time from grid mode to battery mode and vice versa [3, 4].

UPS systems can be categorized as offline, online and line interactive UPS systems [5]. Online UPS systems are most popular and common configuration among them, as it provides isolation to load from the grid and has negligible switching time. Conventional online UPS system consists of rectifier for PFC, battery bank, and an inverter connected to the load [6]. Grid frequency transformers are normally employed to reduce the battery bank voltage and provide isolation from the transients and spikes generated inside the grid. Since the transformer is operating at line frequency, thus increasing the size and weight of the system substantially. Online UPS system with high frequency transformer isolation has been used to overcome the problem related to grid frequency transformer UPS system [7]. Although the size has been reduced, the efficiency of the system decreases due to high number of active switches in these topologies. In order to overcome the problems related to aforementioned topologies, the transformerless UPS system has been introduced. Transformerless UPS systems have comparatively high efficiency, small weight and volume of the system. This makes the transformerless UPS more suitable for environments where the connected grid is less polluted.

Several transformerless topologies has been proposed in [8-11], focusing on efficiency improvement, volume and weight reduction, decreasing the number of switches, and capital cost of the system. But the size of the battery bank in all the proposed systems so far is enormously high. Generally, the batteries are connected in series to achieve high battery bank voltage. But series battery arrangement has major drawbacks and limitations in charging and discharging. Small imbalance in voltages occurs across the battery cells during charging and discharging since battery cells are not equal. Hence, these cannot provide the same performance during operation. Overcharging will

cause severe overheating, low performance, and even destruction [12]. Similarly, deep discharge may cause the battery cell to be damaged permanently [13]. Due to this reason, small battery bank with batteries operating in parallel improves the performance of the battery bank significantly.

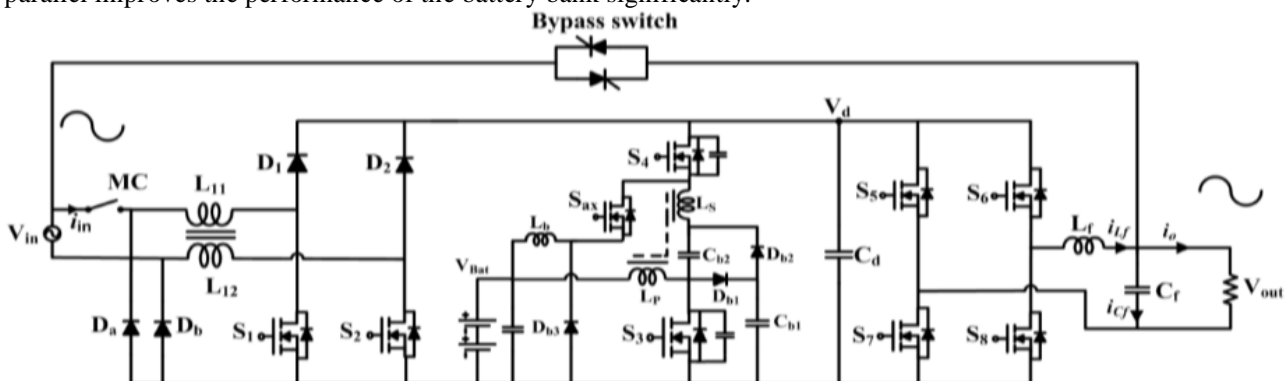


Fig. 1 Circuit diagram of the proposed UPS system

In this paper, a novel transformerless online UPS has been proposed as shown in Fig. 1. The proposed UPS employs a high gain bidirectional converter which operates between the dc-link voltage and battery bank. Using bidirectional charger/discharger, the battery bank is reduced to only 24V (single battery), thus, it eliminates the drawbacks related to large string of series connected batteries. The bridgeless boost rectifier provides the regulated dc-link voltage to feed inverter and maintains the power factor correction. A new controller combining slide mode and proportional-resonant (PR) control has been implemented for the inverter control which shows good performance with low total harmonics distortion (THD) and high stability for both non-linear and impulsive loads. The size and cost of the proposed system is comparatively very low as no bulky transformer has been used, with small battery bank and high efficiency.

II. RELATED WORK

1. **A.Lahyani, P. Venet, A. Guerhazi, and A. Troudi, "Battery/supercapacitors combination in uninterruptible power supply (UPS)," *IEEE Transactions on Power Electronics*, vol. 28, pp. 1509-1522, 2013.** This paper presents a study of the reduction in battery stresses by using Super capacitors (SCs) in UPS. We aim at investigating the optimal Super capacitors-battery combination versus the SCs cost. This investigation is threefold; first, super capacitors and battery models developed using MATLAB/ Simulink are presented and validated. Second, the architecture and the simulation of the designed system that combines the SCs and the battery are shown. The Super capacitors are used as high-power storage devices to smooth the peak power applied to the battery during backup time and to deliver full power during short grid outages. By charging the SCs through the battery at a suitable rate, all impulse power demands would be satisfied by the Super capacitors. Third, extensive simulations are carried out to determine the gain in battery RMS current, the gain in energy losses, the energy efficiency and the elimination rate of surge load power. These four performance parameters are determined by simulation and then analysed.
2. **B. Zhao, Q. Song, W. Liu, and Y. Xiao, "Next-generation multi-functional modular intelligent UPS system for smart grid," *IEEE Transactions on Industrial Electronics*, vol. 60, pp. 3602-3618, 2013.** This project presents a multi-functional Intelligent UPS system for grid, which is composed of a three phase fully controlled rectifier, grid and PV as power source, Lead Acid Battery and an IGBT inverter. Along with the basic functions of a traditional UPS system, the proposed UPS system adds up with a new control strategy that incorporates renewable energy like PV in order to make the system more Greener. The system eliminates the use of buck converter and a new approach for battery charging has been proposed. The operating principle and system configuration of the proposed UPS system are analysed, and control strategies and algorithms are proposed. The proposed system is simulated in MATLAB/SIMULINK and the simulation results verify the credibility and

International Journal of Innovative Research in Science, Engineering and Technology

(A High Impact Factor, Monthly, Peer Reviewed Journal)

Visit: www.ijirset.com

Vol. 7, Issue 4, April 2018

productiveness of the proposed system and its control strategy. This research could assist in acquiring some valuable references in design sectors of next-generation electrical equipment in smart grid.

3. **R. P. Torrico-Bascopé, D. Oliveira, C. G. Branco, and F. L. Antunes, "A UPS with 110-V/220-V input voltage and high-frequency transformer isolation," *IEEE Transactions on Industrial Electronics*, vol. 55, pp. 2984-2996, 2008.** This work deals with the development of a PFC pre-regulator circuit with possibility of 110V/220V ac main input voltages, while maintaining the same efficiency for a wide load range. Other relevant features of this circuit topology are high frequency transformer isolation, soft commutation of the controlled switches, simple control strategy that can be implemented with well-known integrated circuits and the use of few batteries in series due to step-up stage. This circuit is recommended for on-line UPS applications and it is convenient for the development in rack-type structures due to small size and reduced weight. Qualitative analysis and experimental results obtained from 1.6kW prototype are presented.
4. **E.-H. Kim, J.-M. Kwon, and B.-H. Kwon, "Transformerless three-phase on-line UPS with high performance," *IET Power Electronics*, vol. 2, pp. 103-112, 2009.** This paper discusses the design of controller for transformer less uninterruptible power supply (UPS), with simultaneous ac and dc loading. The objective of the design is to maintain good regulation of the ac and dc voltages and sinusoidal inductor currents simultaneously. The volt-second balance across the output filter inductor is used to maintain the current in sinusoidal form which is the unique contribution of this paper. Complete analytical design solution is provided for both rectifier and inverter simultaneously. Implementation of the controller requires simple analog circuits. The proposed solution is validated through simulation and experimentation.

III. PROPOSED SYSTEM DESCRIPTION

The schematic of the proposed single phase online UPS system is shown in Fig. 1. The proposed system consists of a bridgeless PFC boost rectifier, a bidirectional converter, and an H-bridge inverter. The boost rectifier provides the power factor correction and regulated dc-link voltage. The efficiency of the bridgeless rectifier is also high as compared to conventional rectifiers because it eliminates some devices from the power flow path and reduces the conduction losses considerably. Introducing a bidirectional converter for battery charging and discharging with high voltage gain reduces the size of battery bank significantly. The H-bridge inverter with new robust control scheme is proposed for regulating the nonlinear load and provides fast transient response during change of modes

A. Modes of Operation

The operation of the UPS can be divided into two modes of operation. Grid mode and battery mode as shown in the Fig. 2

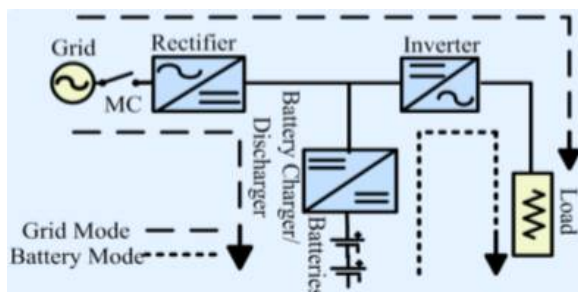


Fig. 2 Modes of operation of proposed UPS system

Grid Mode: When the grid voltage is stable and there is no power failure, the UPS system operates in grid mode. The rectifier provides the regulated dc-link voltage to feed the inverter while the bidirectional converter keeps charging the battery bank.

Battery Mode: In case of power failure or voltage sag at input, the magnetic contactor (MC) is opened and the rectifier is disabled. Then power is supplied to the load by the battery which uses the battery discharger and the inverter. The value of the dc-link capacitor is kept high in order to provide sufficient energy to the inverter during the transition between the battery mode and grid mode of operation.

Bypass switch has been added in the system to increase the reliability of the system. In case of internal fault in the system or overloading and overheating of the circuit, the bypass switch turns ON and provides a direct path for the power from the utility grid to the connected load [2].

B. Bidirectional Converter

A new non-isolated bidirectional dc-dc converter with coupled inductor has been proposed which works as battery charger/discharger and operates between battery bank and the dc-link. The converter has following advantages.

1. Less number of passive components in the circuit.
2. High voltage gain in both the buck and boost mode.
3. Only three active switches are used to perform bidirectional operation.
4. Zero Voltage Switching (ZVS), synchronous rectification, and voltage clamping circuit are used that reduces the switching and conduction losses.

Coupled inductor has been used with L_p as primary inductance and L_s as the secondary inductance. The capacitor C_{b2} inserted in the main power across the primary and secondary windings of the transformer gives high voltage conversion ratio and reduces the peak current stress allowing continuous current in the primary. Also, voltage stress of the capacitor C_{b2} is minimum at this position in the circuit.

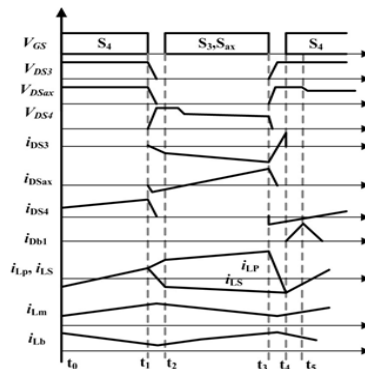


Fig. 3 Characteristic waveforms of the buck mode of operation

1. Buck Operation/Battery Charging

The characteristic waveforms of the converter during battery charging mode are shown in Fig. 3. D_1 is the duty cycle of S_3 and S_{ax} while D_3 is the duty cycle of switch S_4 . Both D_1 and D_3 are related to each other by a relationship $D_1 (= 1 - D_3)$. L_m is the magnetizing inductance of the coupled inductor with turns ratio $N = N_2/N_1$, where N_1 is the number of turns in primary winding and N_2 is the number of turns for secondary winding. The operation of the circuit during battery charging mode in each interval is shown in Fig. 4.

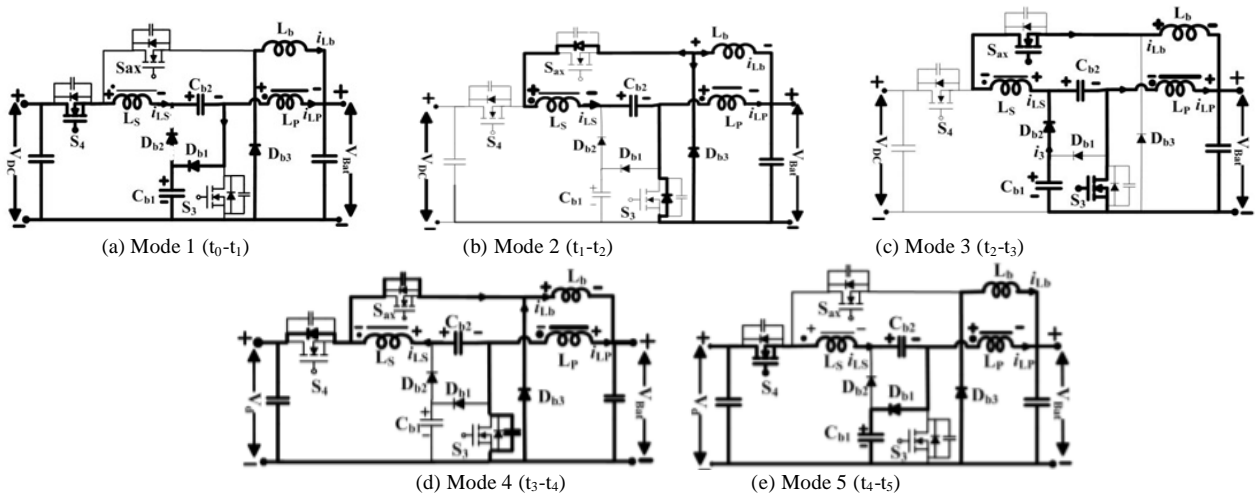


Fig. 4 Topological stages in buck mode: (a) Mode 1; (b) Mode 2; (c) Mode 3; (d) Mode 4; (e) Mode 5

International Journal of Innovative Research in Science, Engineering and Technology

(A High Impact Factor, Monthly, Peer Reviewed Journal)

Visit: www.ijirset.com

Vol. 7, Issue 4, April 2018

Interval 1 ($t_0 \sim t_1$): The Switch S_4 remains ON while the switches S_3 & S_{ax} are OFF during interval 1. The current i_{LS} flows from dc-link to the battery bank through the capacitor C_{b2} and both the windings of the coupled inductor. Applying KVL, we get (1).

$$V_{DC} = V_{LS} + V_{Cb2} + V_{LP} + V_{Bat} \quad (1)$$

$$V_{DC} = V_{LP}(1+N) + V_{Cb2} + V_{Bat} \quad (2)$$

The diode D_{b3} is also conducting with continuous inductor current i_{Lb} into the battery bank. Hence, V_{Bat} is the voltage across inductor L_b .

Interval 2 ($t_1 \sim t_2$): At the start, the switch S_4 turns OFF. Due to the storage energy in the leakage inductor, the polarities are reversed across the primary and secondary windings (L_S & L_P) of the coupled inductor. Switch S_4 is OFF in this mode, but the secondary current i_{LS} is still conducting, so the switch S_{ax} body diode is forward bias in order to keep the current i_{LS} flowing. The diode D_{b3} remains forward biased in this mode. The body diode of switch S_3 gets forward biased as the secondary current i_{LS} decreases, however the primary current i_{LP} remains the same.

Interval 3 ($t_2 \sim t_3$): Both the Switches S_3 and S_{ax} turns ON following zero voltage switching (ZVS) condition. The capacitor C_{b2} starts discharging across battery bank through the switch S_{ax} and inductor L_b . Thus, the secondary current is induced in reverse by discharging capacitor C_{b2} . Clamp capacitor C_{b1} also discharges through the diode D_{b2} by adding small current i_3 into the secondary current flowing into the battery bank.

Using the voltage second balance, V_{Cb2} will be,

$$V_{Cb2} = V_{Lb} + V_{Bat} + V_{LS} \quad (3)$$

The stored energy in the coupled inductor is released by primary current through the switch S_3 into battery bank. Using the voltage-second balance, the V_{Lb} is given by,

$$D_1 V_{Lb} = D_3 V_{Bat} \quad (4)$$

Primary winding voltage V_{LP} can be obtained as,

$$D_3 V_{LP} = D_1 V_{Bat} \quad (5)$$

Putting (4) and the values of V_{Lb} and V_{LP} in (2), the voltage gain during buck mode of operation is given by,

$$G_{buck} = V_{Bat} / V_{DC} = [D_3 (1-D_3)] / [2N (1-D_3)^2 + 1] \quad (6)$$

Interval 4 ($t_3 \sim t_4$): Both the switches S_3 and S_{ax} turn OFF at the start of this mode. The primary and secondary winding currents i_{LP} & i_{LS} will continue conduction due to the leakage inductance of the coupled inductor. The secondary current will charge the parasitic capacitance of the switches S_3 & S_{ax} , and discharge the parasitic capacitance of the switch S_4 . When the voltage across the switch S_{ax} equals to V_d , the body diode of the switch S_4 get forward biased. The primary current i_{LP} starts decreasing unless it gets equal to the secondary current i_{LS} , then this mode finishes.

Interval 5 ($t_4 \sim t_5$): The switch S_4 turns ON under zero voltage switching (ZVS) condition. The capacitor C_{b1} is charges through the clamped diode D_{b1} . The primary and secondary current starts increasing. At the end of this mode, the circuit starts repeating interval 1 of the next cycle.

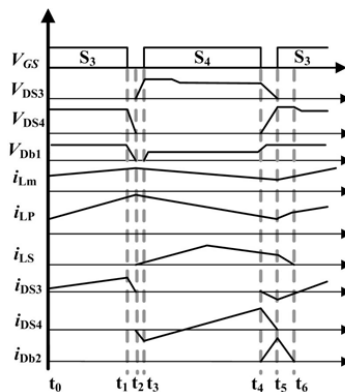


Fig. 5 Characteristic waveforms of the boost mode

International Journal of Innovative Research in Science, Engineering and Technology

(A High Impact Factor, Monthly, Peer Reviewed Journal)

Visit: www.ijirset.com

Vol. 7, Issue 4, April 2018

2. Boost Operation/Battery Discharging

The characteristic waveform of the bidirectional converter during battery discharge mode is shown in Fig. 5. The bidirectional converter steps up the low battery bank voltage to high dc-link voltage. The switch S_{ax} remains OFF during battery discharging. The battery discharger operation during each interval is shown in Fig. 6.

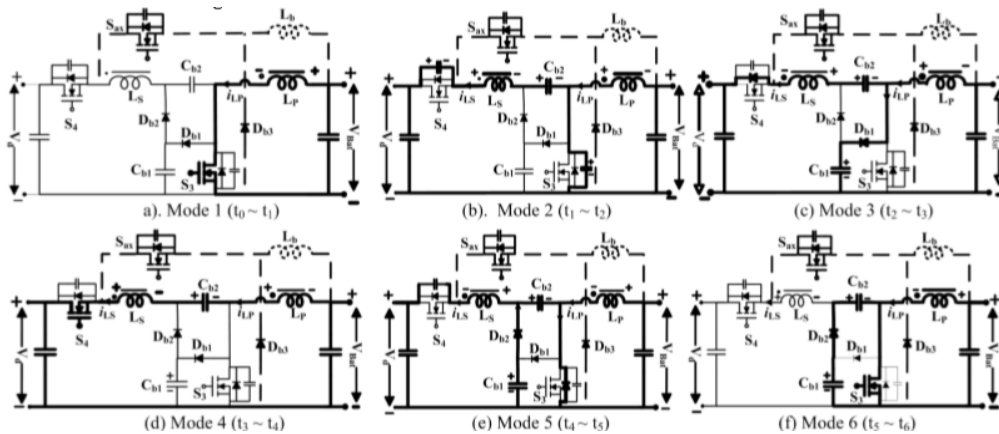


Fig. 6 Topological stages in boost mode: (a) Mode 1; (b) Mode 2; (c) Mode 3; (d) Mode 4; (e) Mode 5; (f) Mode 6

Interval 1 ($t_0 \sim t_1$): During interval 1, the switch S_3 was ON, while the switch S_4 was OFF. Low battery bank voltage is applied at the low voltage side of the circuit. Capacitor C_{b2} remains charged before interval 1 and the magnetizing current i_{Lm} of the coupled inductor increases linearly as shown in the Fig. 5. Applying KVL, we get,

$$V_{Bat} = V_{LP} = V_{LS} / N \tag{7}$$

The voltage across the primary winding can be derived using voltage second balance

$$V_{LP} D_3 = V_{Bat} D_1 \tag{8}$$

Interval 2 ($t_1 \sim t_2$): The switch S_3 turns OFF in interval 2. The primary current i_{LP} charges the parasitic capacitance across the switch S_3 and the secondary current i_{LS} discharges the parasitic capacitance across switch S_4 . When the voltage across switch S_3 becomes equal to the capacitor voltage V_{Cb1} , this interval finishes.

Interval 3 ($t_2 \sim t_3$): Since the switch S_3 is OFF, leakage inductance causes the primary current i_{LP} to decrease while the secondary current i_{LS} increases. As a result, the body diode of switch S_4 gets forward biased. Capacitor C_{b1} starts charging through diode D_{b1} because the voltage across the switch S_3 gets higher than capacitor C_{b1} . This limits the voltage stress across the switch S_3 . The voltage across the C_1 is given by,

$$V_{C1} = V_{Bat} + V_{LP} \tag{9}$$

Using equation (7),

$$V_{C1} = V_{Bat} / D_3 \tag{10}$$

Interval 4 ($t_3 \sim t_4$): The switch S_4 turns ON under the condition of zero voltage switching (ZVS). The primary and secondary windings of the coupled inductor and the capacitor C_{b2} are all now connected in series to transfer the energy to the dc-link. The i_{LS} starts increasing until it reaches the i_{LP} , then it follows the i_{LP} till the end of the interval 4. Thus, the energy stored in the primary and secondary windings discharges across the dc-link. Both the diodes D_{b1} and D_{b2} remain reverse biased during this interval as shown in Fig. 6(d). Using voltage second balance, we get (11)

$$V_{DC} = V_{Bat} + V_{LS} + V_{C2} + V_{LP} \tag{11}$$

$$V_{DC} = V_{Bat} + V_{C2} + (N+1) V_{LP} \tag{12}$$

Interval 5 ($t_4 \sim t_5$): During this interval, the switch S_4 turns OFF. The current i_{LS} charges the parasitic capacitance of the switch S_4 . The capacitor C_{b1} starts discharging across the capacitor C_{b2} , through the diode D_{b2} .

$$V_{Cb2} = V_{Cb1} = V_{Bat} / D_3 \tag{13}$$

By putting (8) and (13) in (12), Voltage gain of the circuit is.

$$V_{DC} = V_{Bat} / D_3 + (N+1) D_1 / D_3 V_{Bat} \tag{14}$$

$$G_{boost} = V_{DC} / V_{Bat} = (2+N D_1) / (1- D_1) \tag{15}$$

The body diode of the switch S_3 starts forward biased because of the polarities of the capacitor C_{b2} and inductor L_P .

International Journal of Innovative Research in Science, Engineering and Technology

(A High Impact Factor, Monthly, Peer Reviewed Journal)

Visit: www.ijirset.com

Vol. 7, Issue 4, April 2018

Interval 6 ($t_5 \sim t_6$): During interval 6, the switch S_3 turns ON under the condition of zero voltage switching. Since S_3 is not deriving any current from the clamped circuit, thus the switching losses remain low due to ZVS and the efficiency of the circuit increases. When both the V_{Cb1} and V_{Cb2} get equal, then the next switching cycle starts and repeats the operation in interval 1.

The turn ratio N is selected as such to satisfy the G_{boost} and G_{buck} gains for required DC-link and battery bank voltage. Fig. 7 shows the voltage gain of buck and boost modes with respect to duty cycle D_3 and D_1 respectively at different turn ratio. Turn ratio $N = 4$ satisfies the operation of bidirectional converter between the required dc-link and battery bank.

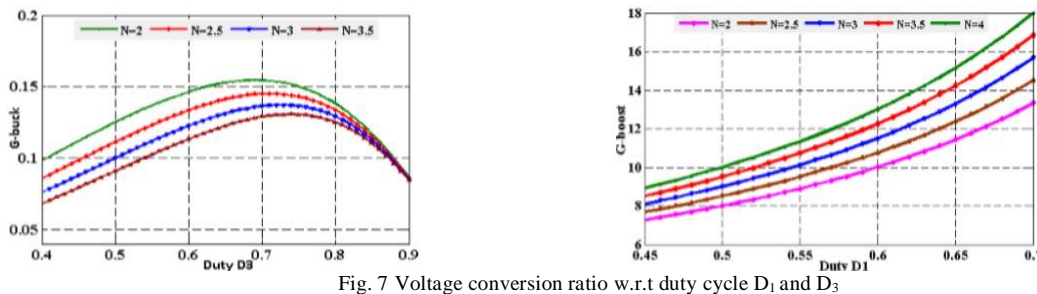


Fig. 7 Voltage conversion ratio w.r.t duty cycle D_1 and D_3

IV. CONTROL STRATEGY

The control scheme for inverter keeps operating in both the grid and battery mode. For rectifier, the control scheme operates only in grid mode, while the battery charger and discharger also switch during the change of modes. The control schemes for controlling different parts of the UPS, in different modes of operation are shown in Fig. 8.

A. Inverter Control

In order to control the output voltage of the inverter, a cascaded control algorithm of SMC (Slide Mode Control) [14] and PR (Proportional Resonant) [15] control has been analysed for the proposed UPS topology. It is a new control scheme for the single phase bipolar voltage source inverter of UPS system. The inner current loop is controlled by the slide mode control while the outer voltage loop is controlled by the PR control. The chattering phenomenon in the SMC is eliminated by using smoothed control law in narrow boundary layer. The smoothed control law applied to the pulse width modulator results in a fixed switching frequency operation of the inverter. Thus, the proposed controller adopted the characteristics of both SMC and PR control. The controller shows good response with low THD and high stability for non-linear loads.

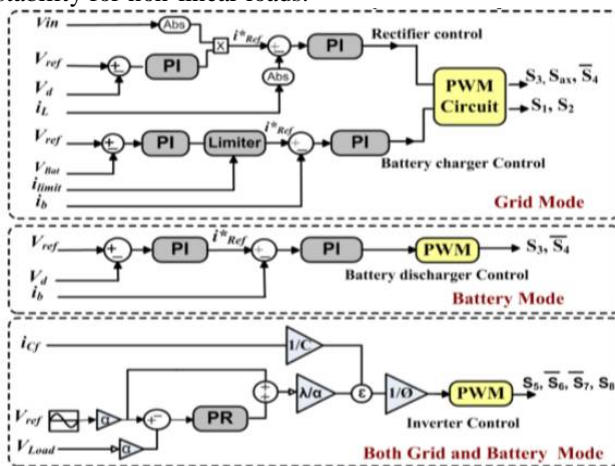


Fig. 8 Control circuit of proposed UPS system

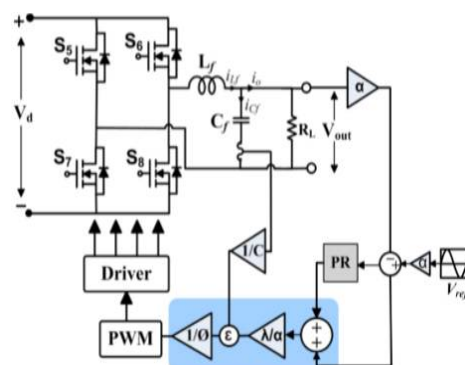


Fig. 9 Block diagram inverter control

International Journal of Innovative Research in Science, Engineering and Technology

(A High Impact Factor, Monthly, Peer Reviewed Journal)

Visit: www.ijirset.com

Vol. 7, Issue 4, April 2018

The circuit diagram of single phase inverter with LC filter and proposed controller for non-linear load is shown in Fig. 9. V_d is applied dc-link voltage, V_{out} the filter capacitor C_f output voltage. i_{L_f} is the inductor L_f current and i_o the output current through the load R, given by $i_o = V_{out}/R$

Sl. No.	Parameters	Value
1	K_p	2.5
2	K_R	30
3	λ	20,000
4	Φ	126830
5	V_m	8V
6	A	0.02227
7	V_{ref}	220V

Table 1. Control Parameters of Inverter

B. Rectifier Control

The rectifier of the UPS system is controlled by well-known average current mode control as shown in Fig. 8. In this control scheme, the faster inner current loop regulates the inductor current so that its average value during each period follows the rectified input voltage. The slower outer voltage loop maintains rectified output voltage close to reference voltage and generates the control signal v_c for the current loop.

C. Battery Charger and Discharger Control

The controller for the battery charger/discharger during both grid mode and battery mode has been shown in Fig. 9. During battery charging, the controller operates as constant current mode (CC) or constant voltage mode (CV) depending on battery voltage while, in battery discharging, the controller regulates the dc-link voltage as well as the primary inductor current. It is assumed that the primary inductor current i_{LP} flows continuously. The steady state analysis of the battery charger/discharger is performed using average state variable method [16]

V. EXPERIMENTAL RESULTS

To verify the performance of the proposed UPS system, a laboratory prototype has been implemented with the specifications shown in Table 2. The design parameters of the rectifier, battery charger/discharger, and inverter are shown in Table 3, Table 4 and Table 5 respectively. The backup storage system consists of two batteries (each battery is 24V/35 Ah), or parallel batteries depending upon the backup time for the connected load

The utility input voltage and current waveform in grid mode of operation is shown in the Fig. 10. The output voltage and current waveform during battery mode and grid mode are as shown in fig 11 and 12 respectively.

Parameters	Symbol	Value
Input voltage	V_{in}	220V
Grid Frequency	V_{out}	220V
Output Frequency	f_r	50Hz
Number of Batteries	V_b	2
Max. Power O/P	V_d	360V

Table 2 Specification of proposed system

Parameters	Symbol	Value
Input inductor	L_{11}, L_{12}	800 μ H
Diodes	D_1, D_2	BYC10-600
Switches	S_1, S_2	SPP11N60C3
Slow Diodes	D_a, D_b	GBJ1508
Switching Frequency	F_s	30000Hz

Table 3 Design parameters of the rectifier

Parameters	Symbol	Value
DC Link voltage	V_d	360V
Battery Bank Voltage	V_b	24V
Switching Frequency	f_s	30,000Hz
Coupling Inductor	C_{b1}, C_{b2}, C_{b3}	$N=4,$ $L_m=107\mu$ H
Switches	S_3, S_4, S_x	MOSFET

Table 4 Specification of battery charger/discharger

Parameters	Symbol	Value
Switching Frequency	f_s	20,000Hz
Switches	S_5-S_8	SPP11N60C3
Output Filter Inductor	L_f	840 μ H
Output Filter capacitor	C_f	6.6 μ F
Cut off Frequency	f_{cut}	17,00Hz

Table 5 Design parameters of inverter

International Journal of Innovative Research in Science, Engineering and Technology

(A High Impact Factor, Monthly, Peer Reviewed Journal)

Visit: www.ijirset.com

Vol. 7, Issue 4, April 2018



Fig. 10 Input voltage and current waveform

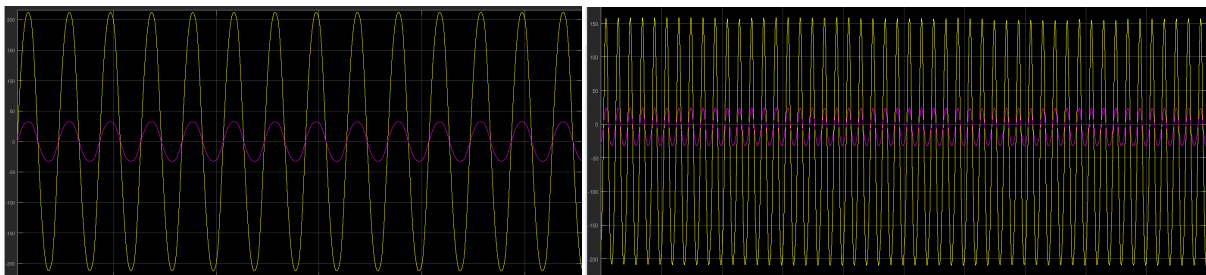


Fig. 11 Output voltage and current waveform during battery mode Fig. 12 Output voltage and current waveform during grid mode

Fig. 13 shows the efficiency graph with maximum efficiency of 94% during battery mode and 92% during grid mode of operation. Thus utilizing soft switching in bidirectional converter reduces the switch losses and increases the efficiency of the system. The efficiency in battery mode is high as compare to grid mode, because less number of power stages are operation during this mode.

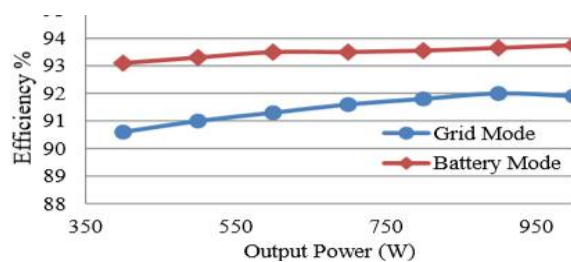


Fig. 13 Efficiency graph in grid and battery mode

VI. CONCLUSION

A single phase transformerless online uninterruptible power supply has been proposed in this paper. A bridgeless boost rectifier has been used with average current control method that increases the efficiency of the system and provides the power factor correction. A new bidirectional converter for battery charging/discharging has been implemented which ensures transformerless operation and reduces the battery bank significantly. A new control for the inverter provides regulated sinusoidal output voltage with low THD for both linear and non-linear load. Overall the volume of the system is minimized by reducing the size, weight, and battery bank of the system. The experimental results show good dynamic and steady state performance. It may be recommended to extend this proposed UPS system to three phase transformerless online UPS system.

International Journal of Innovative Research in Science, Engineering and Technology

(A High Impact Factor, Monthly, Peer Reviewed Journal)

Visit: www.ijrset.com

Vol. 7, Issue 4, April 2018

REFERENCES

- [1] A. Lahyani, P. Venet, A. Guermazi, and A. Troudi, "Battery/supercapacitors combination in uninterruptible power supply (UPS)," *IEEE Transactions on Power Electronics*, vol. 28, pp. 15091522, 2013.
- [2] Y. Zhang, M. Yu, F. Liu, and Y. Kang, "Instantaneous current-sharing control strategy for parallel operation of UPS modules using virtual impedance," *IEEE Transactions on Power Electronics*, vol. 28, pp. 432440, 2013.
- [3] B. Zhao, Q. Song, W. Liu, and Y. Xiao, "Next-generation multifunctional modular intelligent UPS system for smart grid," *IEEE Transactions on Industrial Electronics*, vol. 60, pp. 3602-3618, 2013.
- [4] C. G. Branco, R. P. Torrico-Bascope, C. M. Cruz, and F. de A Lima, "Proposal of three-phase high-frequency transformer isolation UPS topologies for distributed generation applications," *IEEE Transactions on Industrial Electronics*, vol. 60, pp. 1520-1531, 2013.
- [5] S. Karve, "Three of a kind [UPS topologies, IEC standard]," *IEE Review*, vol. 46, pp. 27-31, 2000.
- [6] F. Botterón and H. Pinheiro, "A three-phase UPS that complies with the standard IEC 62040-3," *IEEE Transactions on Industrial Electronics*, vol. 54, pp. 2120-2136, 2007.
- [7] R. P. Torrico-Bascope, D. Oliveira, C. G. Branco, and F. L. Antunes, "A UPS with 110-V/220-V input voltage and high-frequency transformer isolation," *IEEE Transactions on Industrial Electronics*, vol. 55, pp. 2984-2996, 2008.
- [8] E.-H. Kim, J.-M. Kwon, and B.-H. Kwon, "Transformerless three-phase on-line UPS with high performance," *IET Power Electronics*, vol. 2, pp. 103-112, 2009.
- [9] M. R. Reinert, C. Rech, M. Mezaroba, and L. Michels, "Transformerless double-conversion UPS using a regenerative snubber circuit," in *Power Electronics Conference, COBEP'09. Brazilian*, 2009, pp. 564-570.
- [10] S.-B. Lim, H.-J. Lee, J.-P. Lee, Y.-H. Lee, and S.-C. Hong, "A New single phase double-conversion UPS using PWAM method," in *IEEE 6th International Conference on Power Electronics and Motion Control, IPEMC'09*, pp. 2507-2511, 2009.
- [11] Y. Zhan, Y. Guo, J. Zhu, and H. Wang, "Intelligent uninterruptible power supply system with back-up fuel cell/battery hybrid power source," *Journal of Power Sources*, vol. 179, pp. 745-753, 2008.
- [12] H.-S. Park, C.-H. Kim, K.-B. Park, G.-W. Moon, and J.-H. Lee, "Design of a charge equalizer based on battery modularization," *IEEE Transactions on Vehicular Technology*, vol. 58, pp. 3216-3223, 2009.
- [13] Y.-S. Lee and M.-W. Cheng, "Intelligent control battery equalization for series connected lithium-ion battery strings," *IEEE Transactions on Industrial Electronics*, vol. 52, pp. 1297-1307, 2005.
- [14] P. Cortés, G. Ortiz, J. I. Yuz, J. Rodríguez, S. Vazquez, and L. G. Franquelo, "Model predictive control of an inverter with output filter for UPS applications," *IEEE Transactions on Industrial Electronics*, vol. 56, pp. 1875-1883, 2009.
- [15] S.-C. Tan, Y. Lai, and C. K. Tse, "Indirect sliding mode control of power converters via double integral sliding surface," *IEEE Transactions on Power Electronics*, vol. 23, pp. 600-611, 2008.
- [16] R. W. Erickson and D. Maksimovic, *Fundamentals of power electronics: Springer Science & Business Media*, 2001